# Experimental study of gas diffusion layers nonlinear orthotropic behavior

*Marwa* Ouerghemmi, *Christophe* Carral*, and *Patrice* Mele
*Univ. Grenoble Alpes, Univ. Savoie Mont Blanc, CNRS, Grenoble INP, LEPMI, Grenoble, 38000, France*

**Abstract.** One of the most important components of PEMFC is the gas diffusion layer (GDL), owing to its key role in the reactant diffusion, water management, thermal and electron conductivity. Therefore, the GDL must have an optimal stiffness to ensure these transport functions during numerous hydrothermal cycles.
The understanding of its behavior is still a remaining issue. Its orthotropic mechanical behavior requires a series of mechanical characterizations in the plane of the fibers and out of plane. In addition, there are different manufacturing processes for GDL in sheet or roll form to optimize its functional properties. A macro porous layer (MPL) or different PTFE contents might be added by different manufacturers to optimize its performance. In this study, we have performed several mechanical tests differentiating between in plane and out of plane properties in order to characterize different GDLs available on the market. All of the experimental work has been done in the machine (MD) and cross machine direction (CD) according to the fiber orientation. The different GDL types were then classified into categories presenting similar mechanical response.

## 1 Introduction

The PEMFC is subjected to different range of stresses induced by its assembly process and then by its operating conditions, which have a direct impact on its performance and durability [1,2]. Different studies have shown that the response to the mechanical stress is different from a layer to another in the stack [3,4]. Understanding the mechanical response of the GDL to the different stresses it undergoes during operation cycles will help identify the origin of morphological changes that may impact the performance of the PEMFC [5,6]. For example, cyclic compression causes significant and irreversible changes in the GDL's structure and properties, surface morphology and pore size, which inhibit the gas circulation and blocks the water evacuation. Moreover, it induces a nonlinear decrease in the contact electric resistance between the bipolar plate and GDL [7-11].

Some GDLs undergo hydrophobic treatment or have an additional microporous layer for better efficiency. However, during the manufacturing process, several heterogeneities can appear, such as thickness variation or non-homogeneous distribution of the hydrophobic treatment, which makes its characterization difficult besides its orthotropic criterion.

In this study, the experimental behavior of GDLs has been investigated, in both in plane as well as out of plane according to the machine and cross machine directions. The Young moduli, shear moduli and Poisson's ratios were determined. As a perspective of this work, the properties determined will be implemented in a numerical model to predict the different mechanical behavior of the membrane electrode assembly (MEA) different layers.

## 2 Experimental details

### 2.1. Materials

A range of the most commercialized references of GDL has been characterized, from different manufacturers, with varying PTFE content, and exhibiting or not a MPL (Table1). X-ray tomography observations of these different GDLs have been made and are shown in Figure 1.

**Table 1.** Description of GDLs samples

| GDL type | References | PTFE | MPL |
|---|---|---|---|
| Roll | AvCarb EP40<br>SGL 28AA<br>SGL 29AA<br>SGL 36AA<br>SGL 38AA<br>SGL 39AA | 0 | No |
| Roll+PTFE | SGL 28AA-09<br>SGL 28AA-18<br>SGL 28AA-29<br>SGL 28AA-32 | 9 % -30% | No |
| Roll+PTFE +MPL | SGL 22BB<br>SGL 28BB<br>SGL 36BC<br>SGL 39BC | 13%-15% | Yes |
| Sheet | Spectracarb 2050A-0850<br>TorayH060<br>TorayH090 | 0.4-10% | No |

* Corresponding author: christophe.carral@univ-smb.fr

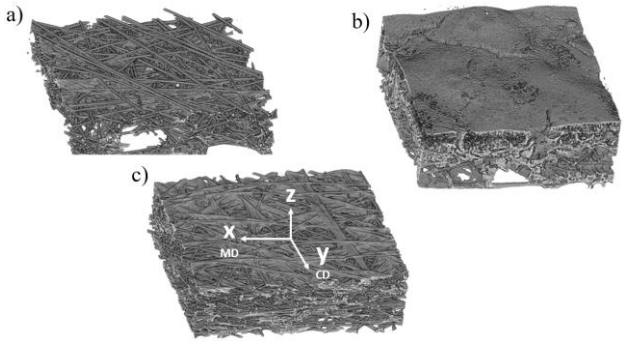


**Figure 1.** Tomographic images of (a) a roll GDL (39AA), (b) a roll GDL with PTFE and MPL (39BC) and (c) a sheet GDL (Toray H090)

## 2.2 Tensile test

The tensile tests were carried out on a Metravib-Acoem VA4000 machine with a 140N force sensor, the displacement speed was 1 mm/min.

A study on the optimization of the sample dimensions was performed during the implementation of the experimental protocol based on the ISO 1924 [12]. This analysis was used to verify the good repeatability of the results. The chosen dimensions for the tensile specimen were 5mm of width and 40mm for the gauged length.

The nominal strain ($\varepsilon_x$) and stress ($\sigma_x$) were calculated with the following equations:

$$\sigma_x = \frac{F_t}{A} \quad (1)$$

$$\varepsilon_x = \frac{\Delta l}{l_0} \quad (2)$$

where $F_t$ is the tensile force, A is the cross sectional area, $\Delta l$ is the change in length and $l_0$ is the initial length.

## 2.3 Poisson's ratio

Tensile tests were carried out on a Shimadzu AGS-X equipped with a video extensometer (Figure 2) to measure the longitudinal and transverse displacements in order to estimate the Poisson's ratio. A force sensor of 100N and displacement speed equals to 1mm/min were employed. The specimens were cut in both MD and CD directions and had a rectangular shape with a width (30mm) greater than that of the tensile tests in order to increase the amplitude of the transverse displacement for the determination of the Poisson's ratio. Tensile tests were performed cyclically: 2 cycles per specimen. The longitudinal and transverse strains were then determined from the changes in the displacements locations of the vertical and horizontal marker points (Figure 3) during the test given by the extensometer, respectively. The displacements were normalized by the initial length values between marks to obtain the strains. It should also be noted that for GDLs with an MPL, tests were carried out on both sides, in order to analyze the possible influence of this layer.

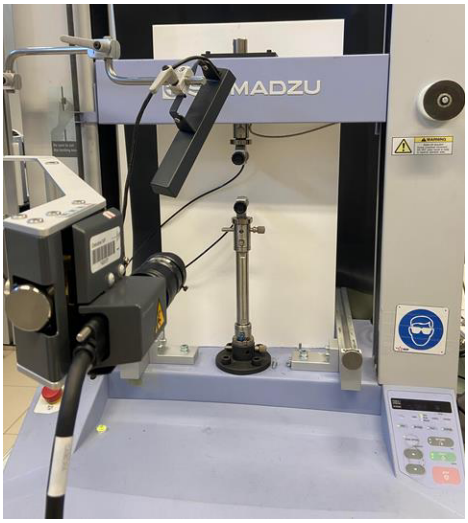


**Figure 2.** Tensile test bench equipped with a video extensometer

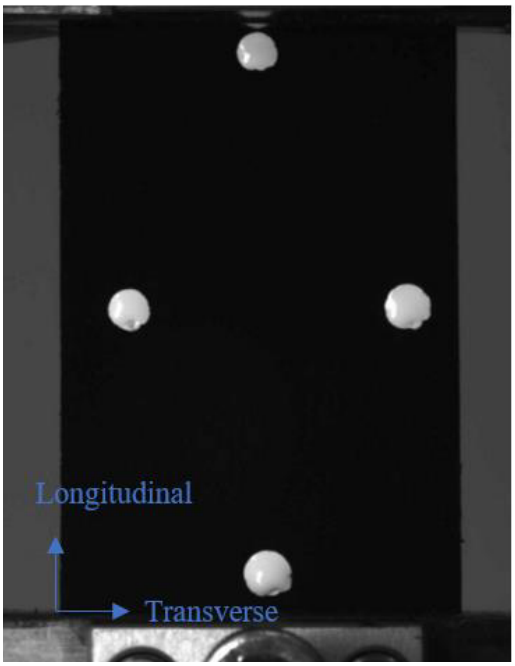


**Figure 3.** Extensometer image of the MPL side on a roll GDL (SGL 22BB)

## 2.4 Shear test

Shear tests were performed on the same machine as the tensile tests with specific in plane and out of plane shear devices (Figures 4 and 5). The out of plane shear test is based on the method described in references [13,14]. Samples were rectangular with dimensions of 30mm×15mm for the in plane shear tests and 30mm×25mm for the out of plane shear test. Shear stress ($\tau$) and strain ($\gamma$) were calculated as follow:

$$\tau = \frac{F_s}{2A} \quad (3)$$

$$\gamma = \frac{d}{g} \quad (4)$$

where $F_s$ is the shear force, A is the cross-sectional area, d is the vertical displacement, and g is the air gap between the jaws. g is equal to 2mm and 0.2mm for the in plane and out of plane shear test set-ups, respectively.

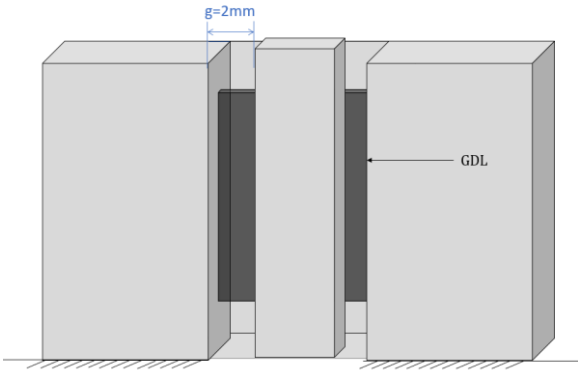


**Figure 4.** Schematic representation of the in-plane shear test

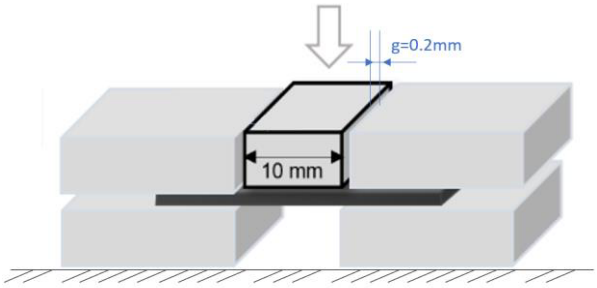


**Figure 5.** Schematic representation of the out of plane shear test

### 2.5 Compression test

The compression tests were carried out on an Instron 8872 machine, equipped with a 5kN force sensor. The displacement was measured with clip-on extensometer installed on the compression plate. Tests were performed on a stack of 6 GDLs of 16 mm diameter, with aluminum spacers of 100 µm thickness (Figure 6). These spacers were used to separate the samples and prevent the interpenetration of carbon fibers.

Only the loading part of the compression of the stack was analyzed with a stress ranging from 0.01MPa up to 20MPa, 0.01 being the contact pressure at which the stack thickness was measured. Compressive stress and strain were calculated as follows:

$$\sigma_z = \frac{F_c}{A} \quad (6)$$

$$\varepsilon_z = \frac{\Delta t}{t_0} \quad (7)$$

where $F_c$ is the compressive force, A is the specimen area, $\Delta t$ is the variation in thickness and $t_0$ is the initial thickness.

The stress can be represented as a function of relative density, as proposed by Carral et al [4]. This representation allows to take into account the fibrous structure of the different GDL.

The relative density $\rho$ can be calculated with the following equation:

$$\rho = \frac{Aw}{t_0(1-\varepsilon_z)\rho_f} \quad (8)$$

where $Aw$ is the areal weight and $\rho_f$ is the fiber density equal to 1.8 g $cm^{-3}$[15].

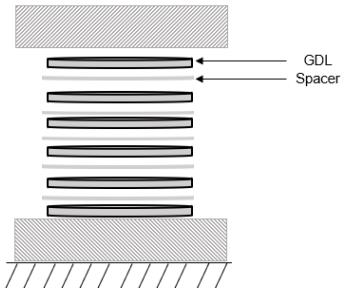


**Figure 6.** Schematic representation of the compression test setup

## 3 Results and discussion

The GDLs exhibit a linear behavior in the MD and CD directions under tensile and shear stresses. Tensile moduli in both directions can be then determined and are shown for the different types of GDL (roll, roll + PTFE, roll + PTFE and MPL and sheet) in Figure 7. The highest elastic properties are obtained for sheets, where a graphitization step is performed on the materials. We can also note the absence of a significant influence of the hydrophobic treatment or the presence of MPL on these properties, for both in plane and out of plane directions. Finally, a weak anisotropy of the elastic properties can be observed with higher properties in the x direction, i.e. in the machine direction.

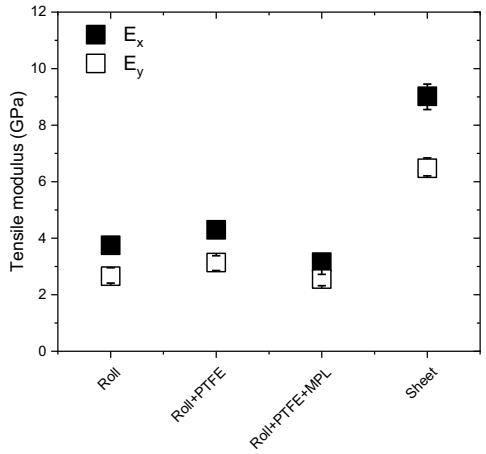


**Figure 7.** Tensile moduli for the different types of GDL

These results are confirmed in Figures 8 and 9 showing the evolution of in plane and out of plane shear moduli for the different types of GDL respectively. We can also notice that the anisotropy of the elastic properties in shear is significant (factor 100) between the in-plane (between 0.1 and 0.3 GPa) and out of plane properties (between 1 and 4 MPa).

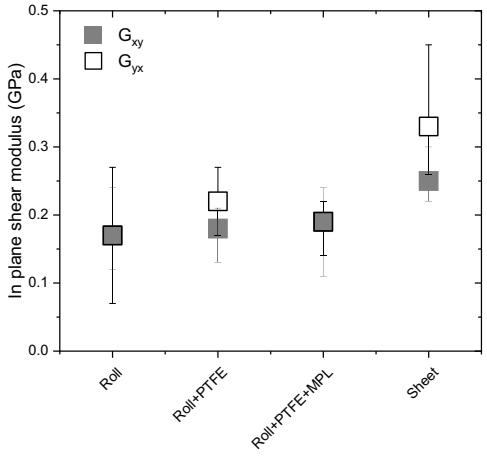


**Figure 8.** In plane shear moduli for the different types of GDL

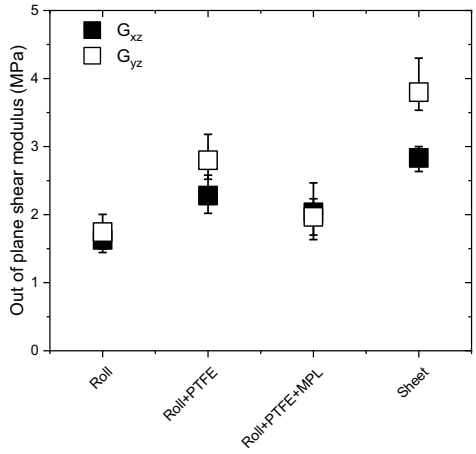


**Figure9.** Out of plane shear moduli for the different types of GDL

### 3.1. Poisson's ratio

The evolution of the transverse deformation as a function of the longitudinal deformation of a roll GDL (SGL 22 BB) on the fibers side and on the MPL side are shown in Figures 10a and 10b, respectively. We can observe a low amplitude of the transverse strain of the GDL on the fibers side (10a) while they are insignificant on the MPL side. This result shows that the GDL with MPL should be considered as a composite structure with different properties. The values of the Poisson's ratio estimated from these curves are collected in Table 2, with values between 0.2 and 0.3 for the fibers part of roll GDLs, and close to 0 for sheets GDL and for the MPL side.

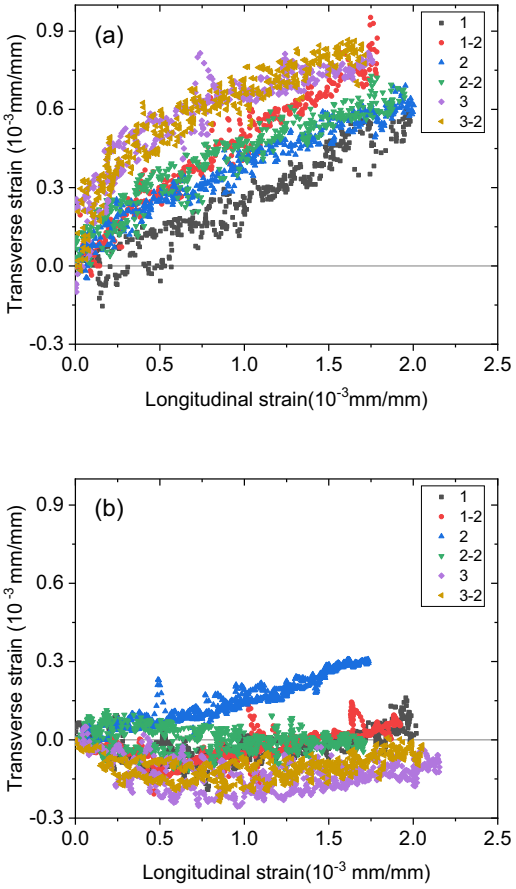


**Figure 10.** Evolution of the transverse strain with the longitudinal strain, (a) on the fibers side and (b) on the MPL side for the reference SGL 22BB in the cross-machine direction

**Table 2.** Values of measured in-plane Poisson's ratio for 2 GDL types (roll/sheet)

| GDL | ν | Fibers | MPL |
|---|---|---|---|
| Roll SGL 22BB | $\nu_{MD}$ | $0.19^{+0.09}_{-0.03}$ | $0.07^{+0.05}_{-0.03}$ |
| | $\nu_{CD}$ | $0.35^{+0.08}_{-0.06}$ | $0.06^{+0.12}_{-0.06}$ |
| Sheet TorayH090 | $\nu_{MD}$ | $\leq 0.05$ | N/A |
| | $\nu_{CD}$ | $\leq 0.05$ | |

### 3.2. Nonlinear compression behavior

The GDL's behavior under compression (out of plane direction) is non-linear (Figure 11). This non-linearity is related to the porous structure of the material, as shown by different authors [16-19]. In fact, the compression leads to the decrease of porosity and therefore the increase of the contacts between fibers.

The results show a minor impact of the hydrophobic treatment under compression loading since the behavior depends mainly on the contact points between the fibers.

From the previous curve, the tangent modulus (Et) is calculated for the different types of GDL and represented in Figure 12 as function of the stress calculated.

Two different regions can be separated from these curves:

- The first region: at stress values below 5 MPa where Et reaches a constant value ranging from 2.5 and 20 MPa for the different types of GDL, this behavior has been linked in the literature to the mechanical history of the GDL during processing [4].

-The second region: at stress values over 5 MPa, linked to the native behavior of GDL for stress greater than the process stress (Figure 13).

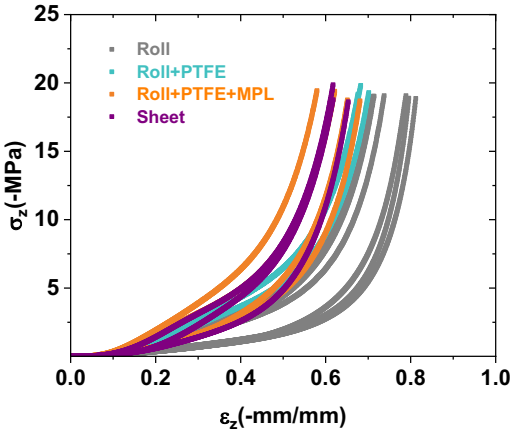


**Figure 11**. Stress-strain curve of the compression test for the different types of GDL

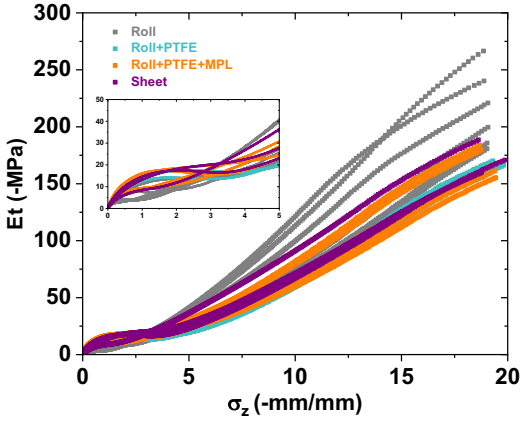


**Figure 12.** Evolution of the tangent modulus vs $\sigma_z$ for the different types of GDL

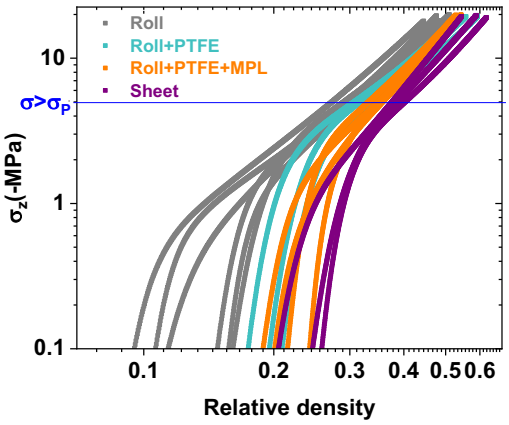


**Figure 13.** Evolution of $\sigma_z$ as a function of relative density for the different types of GDL

## Conclusion

The complex structure of GDL made of dispersed carbon or graphite fibers, requires a meticulous characterization. To study its orthotropic mechanical behavior, we performed a series of mechanical in plane and out of plane tests. The developed method was, then, applied on different types of GDL, from several suppliers. Our reference set included GDLs in sheet and roll form, with different PTFE contents and with or without MPL layer.

All experimental works were performed in the machine and cross machine directions, depending on the fibers orientation.

Through this study, different GDL types were classified into categories depending on their mechanical elastic behavior. Results showed that GDLs in sheet form had a higher in-plane stiffness than GDLs in roll form, under tensile and shear stresses. The non-linear behavior of the GDLs observed under compression was also characterized. The in-plane anisotropy of the GDLs behavior was not significant compared to its anisotropy between the in plane and out of plane directions, the mechanical moduli ranging from several GPa to few MPa respectively.

A specific tensile test was developed in order to determine the Poisson's ratio for the different GDL references, via the use of an extensometer video able to measure the low transverse displacements (few micrometers) of these materials. In our knowledge, for the first time, values of in plane Poisson's ratio of GDLs were thus obtained and presented in this article.

For sheets GDL, and the MPL side of roll GDLs, very low transverse displacements were measured, indicating that the in plane Poisson's ratios for these materials tended to be close to a zero value. A value in the range of 0.2-0.4 was estimated for the in-plane Poisson's ratio of the rolls GDL fibers' part.

In conclusion, this study has enabled the creation of a database of the orthotropic mechanical properties of the most commercially available GDL references allowing the selection of the best GDL for optimized PEMFC performances. These data will also be used to refine the mechanical modelling of PEMFC, by introducing the experimental orthotropic mechanical properties of the different types of GDL.

## References

1. Ozden et al. Progress in Energy and Combustion Science, 2019, 74, 50-102
2. Wu et al. Journal of Power Sources, 2020, 476, 228724
3. Carral et Mélé, International Journal of Hydrogen Energy, 2014, 39, 4516–4530
4. Carral et al., International Journal of Hydrogen Energy, 2018. 43, 19721–19729.
5. Irmscher et al. International Journal of Hydrogen Energy, 2019, 44, 23406–23415
6. Zhang et al. International Journal of Hydrogen Energy, 2020, 45, 23480–23489
7. Radhakrishnan et al. International Journal of Hydrogen Energy,2010, 35, 11107-11118.
8. Bouziane et al. Renewable Energy, 2020, 153, 349–361.
9. Toghyani et al. International Journal of Hydrogen Energy, 2018, 43, 4534–4545.
10. Dafalla et al. International Journal of Hydrogen Energy, 2018, 43, 2327–2348.
11. Zhou et al. Journal of Power Sources, 2017, 163, 874–881.
12. ISO 1924-2: 2008. Paper and board: Determination of tensile properties.
13. Lai et al. Journal of Power Sources, 2008, 184, 120–128
14. Chen et al. Journal of Solid State Electrochemistry, 2019, 23, 2021–2030
15. Mathias et al. Handbook of fuel cells, 42, 2003, 517-37.
16. Norouzifard et al. Journal of Power Sources 2014, 264, 92-99.
17. Kleemann et al. Journal of Power Sources 2009;190, 92-102.
18. El Oualid et al. International Journal of Hydrogen Energy, 2017, 42, 23920-23931.
19. Escribano et al. Journal of Power Sources, 2006, 156, 8-13.